FPO-Based Shooting and Bouncing Ray Method for Wide-Band RCS Prediction

Y. An, Z. Fan, D. Ding, and R. Chen

Department of Communication Engineering
Nanjing University of Science and Technology, Nanjing, 210094, China
eechenrs@njust.edu.cn

Abstract ─ The fast physical optics (FPO) method for calculating the monostatic radar cross section (RCS) of an object over a range of frequencies is extended to the shooting and bouncing rays (SBR) method where the multi-bounce phenomena of the launched rays is considered. The FPO method is an improved version of the physical optics (PO) method, which is efficient when calculating the monostatic RCS over a wide range of frequencies or/and angles. The SBR method, based on the combination of geometrical optics (GO) and PO methods, can reach a higher accuracy compared with the PO method. However, due to different length of ray tube paths, it is difficult to implement the phase compensation and phase retrieval in the SBR as that in the FPO method. In this paper, a coordinate transformation is introduced in the integral equation, which transforms the original ray tubes model into a new one. The FPO technique can then be taken on the revised model without difficulty. The validity and efficiency of the proposed method are validated though a couple of numerical experiments.

Index Terms - Coordinate transformation, electromagnetic scattering, fast physical optics (FPO), shooting and bouncing rays (SBR), and wide-band RCS.

I. INTRODUCTION

The radar cross section (RCS) is an important characterization of the electromagnetic scattering properties of large objects and it is common practice to use this data in the fields of war monitoring, radar imaging simulation, and target identification. Techniques for computing RCS can be categorized into high-frequency techniques and low-frequency techniques [1]. The low-frequency techniques include the method of moments (MoM) [2], the finite element method (FEM) [3] and other MoM-type methods [4-10]. The high-frequency techniques include the geometrical optics (GO) and physical optics (PO) [11] methods, and more complicated methods, such as ILDCs [12], GO/UTD-PO/PTD [13], and SBR [14]. The high-frequency techniques, usually based on the ray-tracing and edge diffraction, are fast and accuracy acceptable when used to electrically large objects [15]. For example, an aircraft at *L* wave band will up to 130 wavelengths, which will result a large number of unknowns if 0.1 wavelength mesh size is used in the MoM method. This large number of unknowns puts forward high demanding in computer performance. However, the high-frequency techniques express the scattering field in an analytical approach and avoid solving the matrix equations as that in the low-frequency techniques, which reduces the memory and CPU time cost significantly.

A lot of researchers have paid attention to the calculation of wide-band RCS of an object. The asymptotic waveform evaluation (AWE) [16-18] technique and model-based parameter estimation (MBPE) [19] have been developed to decrease the computation burden associated with repeated point-by-point calculations [18]. However, the techniques mentioned above are based on low-frequency techniques, and the objects analyzed are not electrically large. Recently, a fast physical optics (FPO) [20-25] has been developed to fast evaluate wide-band or/and wide-angle monostatic RCS. The algorithm is based on the observation that the scattering pattern of a finite scatterer is an

Submitted On: January 23, 2013
Accepted On: March 8, 2014

essentially band limited function of the aspect angles and frequencies [20, 26]. In the FPO method, the rapid oscillation of the integrand is cancelled by a phase compensation process, the RCS response over a range of frequencies or angles can then be obtained by interpolating the phase-compensated field at much sparser sampling grids. The backscattering echo of a 2-dimensional rectangular cylinder [20] and double-bounce scattering phenomena involving two surfaces [21] have been analyzed by the FPO. However, the method is rather complicated and limited to double-bounce scattering phenomena.

The shooting and bouncing rays (SBR) [14], proposed by H. Ling etc., is a robust and an accurate method in analyzing electrically large objects. In the SBR approach rays representing the incident fields in a GO manner are used to determine the resulting equivalent surface currents and finally the resulting field contributions at the given observation points are derived by PO integration [27]. Besides the first-order scattered fields, the SBR provides more accurate results by including the scattered fields arising from multiple bounces [29]. In [29], a GPU-based SBR that implemented on the graphics processing unit (GPU) is proposed to reduce the computation time. The ray tracing is modified to evaluate the exit point and field quickly. The electromagnetic computing is integrated into the process of central ray tracing, including the evaluation of the reflected and scattered field. The main contribution of this paper is utilizing the GPU to accelerate both ray tracing and electromagnetic computing of the SBR, which is a parallelization of the SBR method under a certain frequency and incident angle. The wide-band and wide-angle monostatic RCS can then be obtained by repeating this process at different frequencies and angles. Whereas the method proposed in [20] is focused on getting wide-band or/and wide-angle monostatic RCS with interpolation technique. According to this method, only a few monostatic RCS need to be calculated directly, the RCS at required frequencies and angles can then be obtained by interpolating these calculated ones.

In this paper, the FPO method for calculating the monostatic RCS of an object over a range of frequencies is extended to the SBR method. Unlike the method in [29], the method proposed in this paper tries to get wide-band RCS by interpolating values calculated at sampling frequencies. The RCS at these sampling frequencies can be obtained by either a CPU-based or a GPU-based SBR method as that in [29]. However, due to different length of ray tube paths, it is difficult to implement the phase compensation and phase retrieval in the SBR as that in the FPO method. To conquer this problem, a coordinate transformation is introduced in the integral equation, which transforms the original ray tubes model into a new one. The FPO technique can then be taken on the revised model. The remainder of this paper is organized as follows. In section II, theory and formulations are discussed. Numerical results are presented and discussed in section III. Section IV concludes this paper. The time factor $e^{j\omega t}$ is assumed and suppressed throughout this paper.

II. THEORY AND FORMULATION

Consider a perfectly electrically conductor (PEC) shown in Fig. 1, a plane wave is incident on this object ($\vec{E}_{in}$ and $\vec{H}_{in}$ denote the electric and magnetic field of the incident wave, respectively). *Ro* is half of the diagonal line of the cube that contains the object. To facilitate analysis, the object is meshed with small patches (for example, triangular patches), the number of meshed triangles of which is dependent on the frequency and the size of the object. In section A below, the theory of the FPO is briefly discussed. The SBR and its improvement are discussed in section B.

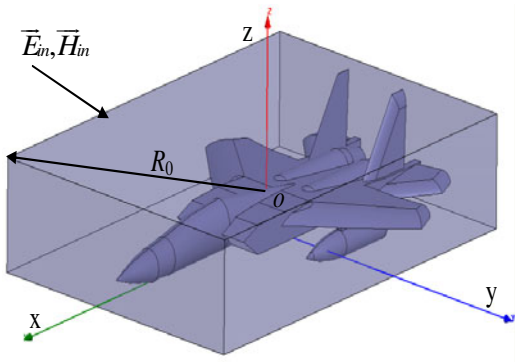

Fig. 1. Scattering model of an object.

A. FPO

As shown in Fig. 1, according to the PO method, the back-scattered field of the object at a fixed frequency can be written as,

$$\vec{E}_s(f) = 2jk\eta \frac{e^{-jkR}}{4\pi R} \sum_{i=1}^{N_t} \int_{s_i} \hat{s} \times [\hat{s} \times (\hat{n} \times \vec{H}_{in})] e^{2jk\hat{s}\cdot\vec{r}'} ds' \quad (1)$$
$$= 2jk\eta \frac{e^{-jkR}}{4\pi R} \sum_{i=1}^{N_t} \int_{s_i} p e^{2jk\hat{s}\cdot\vec{r}'} ds',$$

where $\hat{n}$ is a unit outward normal vector at the point $\vec{r}'$, $\hat{s}$ is the unit vector in the direction of observation. k is the wavenumber, η is the intrinsic wave impedance, N_t is the number of triangle patches in the illuminative area, R is the distance between the observation point and the object, and $j = \sqrt{-1}$. In the high frequency region, k is a large number, and function p is a slowly varying function regarding frequencies. In this paper, the integral technique proposed by Gordon [30] is adopted to calculate the integral in equation (1).

When used to wide-band scattering problems (for example, the required frequency band is $[f_{\min}, f_{\max}]$ with frequency interval Δf), one has to repeat the calculation of equation (1) at a sequence of frequency samples, which is time-consuming when used to electrically large object. According to the Nyquist sampling theorem, the sampling interval of the frequency should satisfy $\Delta f' < c/(4R_o)$, where c is the velocity of light. Consequently, the number of frequency samples is,

$$N_f = \Omega_f 4R_o(f_{\max} - f_{\min})/c, \quad (2)$$

where Ω_f is the oversampling ratio satisfying $\Omega_f > 1$. It is observed that the number of frequency samples is proportional to the size of the object R_o. One possible way to reduce the N_f is by dividing the object into several non-overlapped groups as shown in Fig. 2. The N_f^i of the i-th group is obtained by substituting R_o with R_o^i in equation (2). Since $R_o^i < R_o$, the sampling points $N_f^i < N_f$. The back-scattered field of each group at the required frequencies can then be interpolated by these sparser sampling grids. However, the scattered field obtained by direct interpolation is not accurate. To improve the interpolation accuracy, phase compensation is applied to the back-scattered field prior to interpolation, and a phase retrieval algorithm is used after the interpolation stage. The phase compensated field of the n-th group can be written as,

$$\tilde{\vec{E}}_s^n(f) = 2jk\eta \frac{e^{-jkR}}{4\pi R} \sum_{i=1}^{N_t^n} \int_{s_i} p e^{2jk\hat{s}\cdot(\vec{r}' - \vec{r}_c^n)} ds', \quad (3)$$

where N_t^n is the number of triangle patches in the illuminative area of the n-th group, $\vec{r}_c^n$ is the center coordinate of the n-th group. The rapid oscillation of the integrand is cancelled by the phase compensation process, which makes the interpolation process more accurate. After interpolation, the back-scattered field of each group at the required frequency point can be retrieved by phase restoration, i.e.,

$$\vec{E}_s^n(f) = \tilde{\vec{E}}_s^n(f) e^{2jk\hat{s}\cdot\vec{r}_c^n}. \quad (4)$$

The total back-scattered field $\vec{E}_s(f)$ can then be obtained by aggregation of the back-scattered field of all groups and the monostatic RCS can then be written as,

$$RCS(f) = \lim_{R\to\infty} 4\pi R^2 \frac{|\vec{E}_s(f)|^2}{|\vec{E}_{in}(f)|^2}. \quad (5)$$

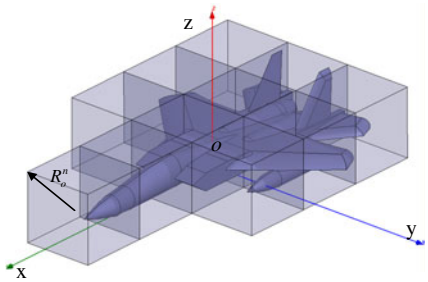

Fig. 2. Schematic drawing of partitioning of the object.

B. SBR and its improvement

The SBR method involves two steps: ray tube tracing and electromagnetic computing at the exit point. First, the incident plane wave is modeled as a dense grid of ray tubes at a virtual aperture, which are shot toward the object. When used to wide-band RCS prediction, the number of ray tubes is set according to the highest frequency to be analyzed. Each ray tube is recursively traced to obtain the exit position and its scattered field. Figure 3 shows a possible path of a ray tracing. It

should be noted that the ray tracing process is time-consuming when the object is meshed with large number of triangles and when the number of ray tubes is large. In [28], the angular Z-buffer (AZB), the volumetric space partitioning (SVP) and the depth-limited search method are combined to accelerate the ray tracing process, whereas a stackless kd-tree traversal algorithm is adopted to evaluate the exit position and field quickly in [29]. In this paper, the octree [31-32] technique is used to recursively subdividing the box into eight children to decrease the number of intersection tests. Second, the PO integral is preformed to obtain the scattered field of this ray tube based on the pre-calculated exit positions and field [29]. The scattered field of the object can be written as,

$$\vec{E}_s(f) = jk\eta \frac{e^{jkR}}{4\pi R} \sum_{i=1}^{N_r} \int_{s_i} \hat{s} \times [\hat{s} \times (\hat{n} \times \vec{H}_i) e^{-jkr_i}] e^{jk\hat{s}\cdot\vec{r}'} ds', \tag{6}$$

where N_r is the number of ray tubes, $\vec{H}_i$ is the magnetic field of the *i*-th ray tube at the exit point, and r_i is the length of the path of the *i*-th ray tube. It can be seen from equations (6) and (1) that both of the two equations have the same format except for the exponential term e^{-jkr_i}. However, due to different length of ray tube paths r_i, it is difficult to implement the phase compensation and phase retrieval in the SBR as that in the FPO method. Furthermore, as mentioned in section II A, that the phase compensation and phase retrieval is applied group by group, not ray by ray. Consequently, the FPO technique can not be used into SBR directly.

We rewrite the exponential terms in equation (6) as,

$$e^{-jkr_i} e^{jk\hat{s}\cdot\vec{r}'} = e^{-jk\hat{s}\cdot\vec{r}_i'} e^{jk\hat{s}\cdot\vec{r}'} = e^{jk\hat{s}\cdot(\vec{r}'-\vec{r}_i')}, \tag{7}$$

where $k\hat{s}\cdot\vec{r}_i' = kr_i' \cos\alpha$, with α as the angle between $\hat{s}$ and $\vec{r}_i'$. In principle, there are various $\vec{r}_i'$ that satisfy this condition. In this paper, we choose $\vec{r}_i'$ as the direction of $\hat{s}$ as shown in Fig. 3, which leads to $\alpha = 0^0$ and $|\vec{r}_i'| = r_i$. Substituting equation (7) into equation (6) we can arrive at,

$$\vec{E}_s(f) = jk\eta \frac{e^{jkR}}{4\pi R} \sum_{i=1}^{N_r} \int_{s_i} \hat{s} \times [\hat{s} \times (\hat{n} \times \vec{H}_i)] e^{jk\hat{s}\cdot(\vec{r}'-\vec{r}_i')} ds'. \tag{8}$$

Let $\vec{r}'' = \vec{r}' - \vec{r}_i'$ and substitute it into equation (8) we finally get,

$$\vec{E}_s(f) = jk\eta \frac{e^{jkR}}{4\pi R} \sum_{i=1}^{N_r} \int_{s_i} \hat{s} \times [\hat{s} \times (\hat{n} \times \vec{H}_i)] e^{jk\hat{s}\cdot\vec{r}''} ds''. \tag{9}$$

The equation $\vec{r}'' = \vec{r}' - \vec{r}_i'$ implies that the final integral can be taken on a new model that moves the exit points in the reverse direction of $\hat{s}$. Comparison between equations (6) and (9) shows that the coordinate transformation extracts the exponential term in the square brackets and combines with the exponential term outside the square brackets. As shown in Fig. 3, the original integral of equation (6) at the exit point (Point C) can be replaced by the integral of equation (9) at point D. In other words, the new model (or integral domain) has taken into account the effect of path of each ray tube, whereas the original integral is taken at the exit point. However, the coordinate transformation does not affect the fields and the medium through the transformation because equation (9) is consistent with equation (6) in essence and there is only a change in variables. To make this clearer, we consider a dihedral corner reflector as shown in Fig. 4 (a), the incident and observation angles are $\theta_i = 45^0$, $\varphi_i = 0^0$, $\theta_s = 45^0$, $\varphi_s = 0^0$. After ray tracing and coordinate transformation, the integral of equation (9) is taking on a new model as shown in Fig. 4 (b). Then the new model can be regrouped without difficulty and take the FPO technique as in section II A to fast get the wide-band RCS prediction.

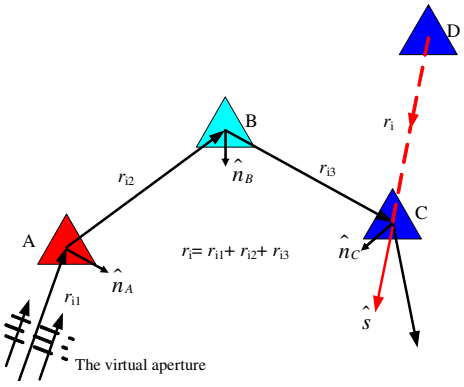

Fig. 3. Schematic drawing of the path of a ray tube.

Points A, B, and C are intersection points during the ray tracing. Point D is obtained by moving point C in the reverse direction of $\hat{s}$ such that the distance between C and D (remarked as r_i) satisfies $r_i = r_{i1} + r_{i2} + r_{i3}$.

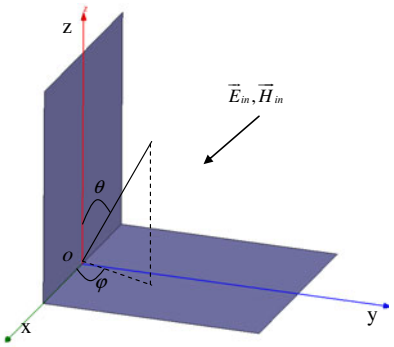

(a)

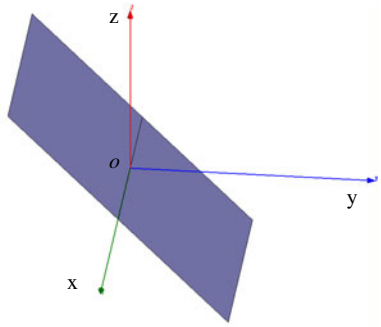

(b)

Fig. 4. Schematic drawing of scattering model of a dihedral corner reflector; (a) the dihedral corner reflector and (b) the new model after ray tracing and coordinate transformation.

III. NUMERICAL RESULTS

In this section, the approach and its efficiency are validated through a couple of numerical experiments. The program is implemented on a personal computer with Intel Dual-core CPU. The CPU and memory sizes are 2.99 GHz and 3.24 GB, respectively. In all examples below, the 4-point Lagrange interpolation technique is used in the FPO with evenly distributed sampling points. As mentioned above, the octree grouping technique is used to accelerate the ray tracing process in the SBR and regrouping is needed on the new model after the ray tracing process. Let l_1 denote the finest group size of the former while l_2 denote the group size of the latter step.

Firstly, we consider a trihedral corner reflector with a side length of $1m$, the geometry of the trihedral corner reflector is shown in Fig. 5. The monostatic RCS on the $\theta = 60^0$ plane is calculated. The virtual aperture is also meshed with 0.01λ as that in [29]. The results of the HH-polarization at 3 GHz are shown in Fig. 6, which show a good agreement between the method proposed in this paper and the method in [29]. The total computation time of the proposed method in this paper is about 281 seconds, whereas the GPU-based method in [29] only needs 8.73 seconds. The reason is that the method introduced in this paper mainly deals with wide-band RCS prediction. The result may become unacceptable when used to wide-angle problems because of the drastic change in the path of each ray tube at different angles. So the proposed method in Fig. 6 degenerates to the conventional SBR indeed. However, as mentioned in the introduction, the GPU-based SBR method in [29] can be combined together with the method proposed in this paper to accelerate the computation at sampling frequencies when dealing with wide-band RCS problems.

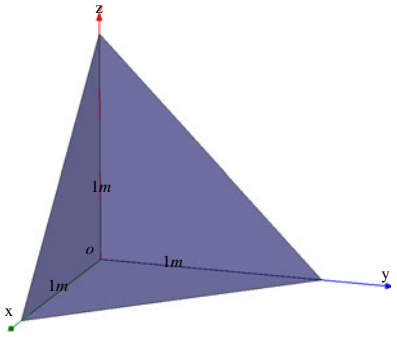

Fig. 5. The geometry of a trihedral corner reflector.

Secondly, we validate accuracy of the proposed method. As shown in Fig. 7, we consider a trihedral corner reflector with a side length of 10 meters. The number of ray tubes is set to be 68,730. The incident angles are $\theta_i = 45^0, \varphi_i = 45^0$, respectively. $l_1 = l_2 = 0.4m$. The frequency range of interest is 0.5 GHz – 1.5 GHz, with frequency interval Δf =20 MHz (resulting 51 frequencies points). By using equation (2) with $\Omega_f = 2$ and

$R_o = \sqrt{3}l_2/2$, only 10 frequencies points are needed to be calculated. Figure 8 is the monostatic RCS for VV polarization versus the frequency. The result simulated by the commercial software CST [33] is also shown in the figure, which shows a good agreement among these methods.

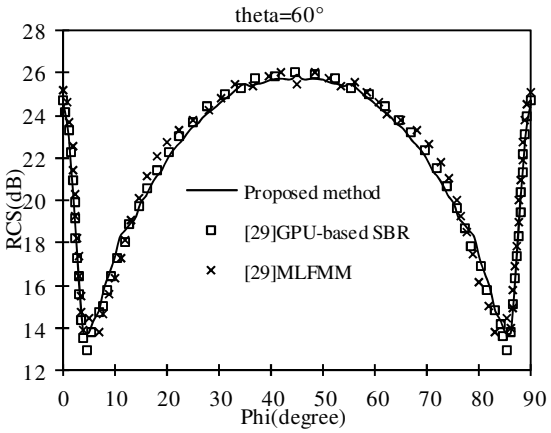

Fig. 6. Comparison of our proposed method and the method in [29] for the trihedral corner reflector.

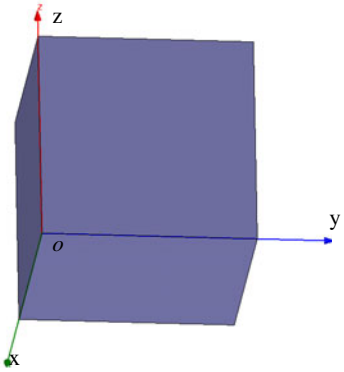

Fig. 7. The geometry of a trihedral corner reflector.

Thirdly, we consider an F15 aircraft as shown in Fig. 1, the size of the F15 aircraft is $4.78m \times 3.35m \times 1.06m$. The incident angles are $\theta_i = 120^0$, $\varphi_i = 0^0$, respectively. The frequency range of interest is 1 GHz − 15 GHz, with frequency interval Δf = 20 MHz (resulting 701 frequencies points and 627,592 ray tubes). $l_1 = l_2 = 0.1m$. Figure 9 is the monostatic RCS for VV polarization versus the frequency with different oversampling rates of the proposed method, which shows a good agreement with the direct SBR method. Table I lists the CPU time and relative error of the proposed method, where the CPU time cost by the ray tracing is not considered (Because the CPU time for the ray tracing are the same for all of the 4 cases). The relative error is given by,

$$relative\ error = \frac{\sum_{i=1}^{frequency\ points} |RCS_{omega} - RCS_{SBR}|_i}{\sum_{i=1}^{frequency\ points} |RCS_{SBR}|_i}, \quad (10)$$

where the RCS calculated by the SBR method is used as the correct solution. It can be seen from the table that the proposed method can reduce the CPU time significantly with reasonable oversampling rates, and the relative error decreases with the oversampling rate increases.

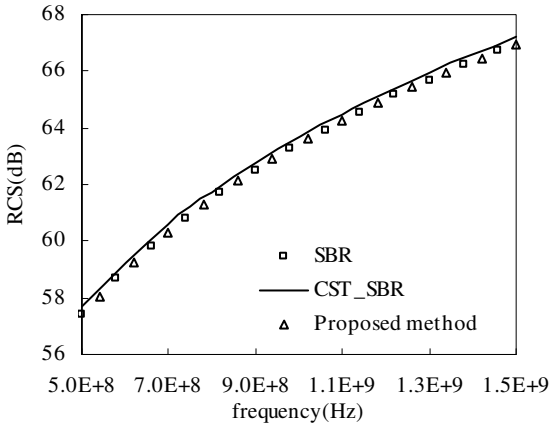

Fig. 8. Monostatic RCS of the trihedral corner reflector versus the frequency computed by the proposed method, the direct SBR method, and commercial software CST. The SBR technique in CST is adopted in the simulation.

Table I: CPU time cost and relative error for different oversampling rates.

	Ω_f	No. of frequency points	CPU time (Sec.)	relative error
SBR	——	701	433	——
Proposed method	$\Omega_f = 2$	34	18	5.6%
	$\Omega_f = 3$	50	26	4.7%
	$\Omega_f = 4$	68	35	4.4%

Finally, we consider a tank model as shown in Fig. 10. The size of the tank is $8.11m \times 2.59m \times 1.82m$. 690,454 ray tubes is used to get an accurate result over the C, X, and

Ku wave band (i.e., 4 GHz – 18 GHz). The frequency interval of interest is Δf =10 MHz. The incident angles are $\theta_i = 60^0$, $\varphi_i = 0^0$. $l_1 = l_2 = 0.1m$ is adopted as that in the third example. Figure 11 shows the monostatic RCS versus the frequency with different oversampling rates of the proposed method, which shows a good agreement with the conventional SBR method. Table II lists the CPU time and error values of the proposed method, from which we can see that the proposed method can reduce the CPU time with a factor of 26 ~44 without losing accuracy compared with the conventional SBR. In terms of relative error, the error values in Table I are higher than those in Table II. The reason is that the monostatic RCS in Fig. 9 is much smaller than that in Fig. 11. The error values can be reduced by a double precision or higher order interpolation technique.

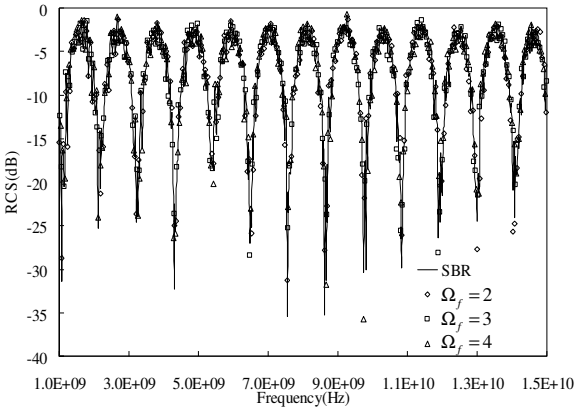

Fig. 9. Monostatic RCS versus frequency computed by the proposed method with different oversampling rates and the SBR method.

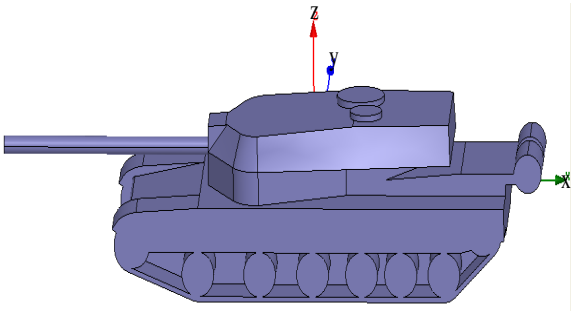

Fig. 10. The geometry of a tank model.

Table II: CPU time cost and relative error for different oversampling rates.

	Ω_f	No. of frequency points	CPU time (Sec.)	relative error
SBR	——	1401	711	——
Proposed method	$\Omega_f = 2$	33	16	0.0972%
	$\Omega_f = 3$	49	22	0.0867%
	$\Omega_f = 4$	65	27	0.0865%

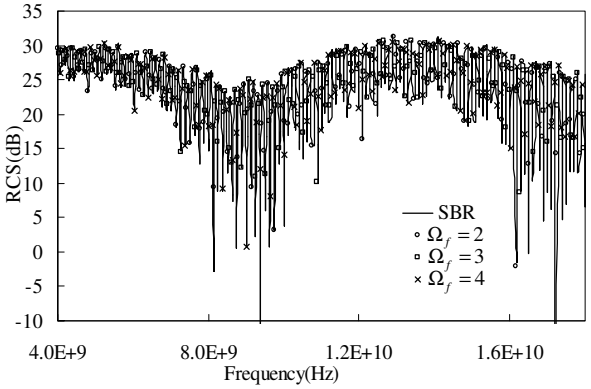

Fig. 11. Monostatic RCS versus frequency computed by the proposed method with different oversampling rates and the SBR method.

IV. CONCLUSION

In this paper, the FPO method for calculating monostatic RCS of an object over a range of frequencies is extended to the SBR method where the multi-bounce phenomena of the launched rays are considered. A coordinate transformation is used to cancel the influence of different length of ray tubes on phase compensation and phase retrieval, which transforms the original integral model into a new one. The FPO technique can then be taken on the revised model without difficulty. The proposed method and its efficiency are validated by numerical experiments, which show that the proposed method can reduce the CPU time significantly. The proposed method is especially suited for generation of synthetic data for radar imaging simulation.

ACKNOWLEDGMENT

This work is partially supported by Natural Science Foundation of 61271076, 61171041, 61371037, Jiangsu Natural Science Foundation of BK2012034, and Ph.D. Programs Foundation of

Ministry of Education of China of 20123219110018. The author would like to thank the reviewers for their comments and suggestions.

REFERENCES

[1] J. Jin, S. Ni, and S. Lee, "Hybridization of SBR and FEM for scattering by large bodies with cracks and cavities," *IEEE Trans. Antennas Propag.*, vol. 43, no. 10, pp.1130-1139, 1995.

[2] R. Harrington, *Field Computation By Moment Methods*, Macmillan, New York, 1968.

[3] J. Jin, *The Finite Element Method In Electromagnetics*, Wiley, New York, 1993.

[4] W. Chew, J. Jin, E. Michielssen, and J. Song, *Fast And Efficient Algorithms In Computational Electromagnetics*, Artech House, Boston, 2001.

[5] E. Michielssen and A. Boag, "A multilevel matrix decomposition algorithm for analyzing scattering from large structures," *IEEE Trans. Antennas Propag.*, vol. 44, no. 8, pp.1086-1093, 1996.

[6] L. Tsang and Q. Li, "Wave scattering with UV multilevel partitioning method for volume scattering by discrete scatters," *Microw. Opt. Technol. Lett.*, vol. 41, no. 5, pp. 354-361, 2004.

[7] E. Bleszynski, M. Bleszynski, and T. Jaroszewicz, "AIM: Adaptive integral method for solving large-scale electromagnetic scattering and radiation problems," *Radio Sci.*, vol. 31, pp. 1225-1251, 1996.

[8] Z. Liu, R. Chen, J. Chen, and Z. Fan, "Using adaptive cross approximation for efficient calculation of monostatic scattering with multiple incident angles," *Applied Computational Electromagnetics Society (ACES) Journal*, vol. 26, no. 4, pp. 325-333, 2011.

[9] H. Fangjing, N. Zaiping, and H. Jun, "An efficient parallel multilevel fast multipole algorithm for large-scale scattering problems," *Applied Computational Electromagnetics Society (ACES) Journal*, vol. 25, no. 4, pp. 381-387, 2010.

[10] M. Pavlovic, B. Mrdakovic, D. Sumic, and B. Kolundzija, "Simulating large RCS problems with MLFMM applied to higher order basis functions implemented in WIPL-D Pro," *25th Annual Review of Progress in Applied Computational Electromagnetics (ACES)*, Monterey, California, pp. 559-564, March, 2009.

[11] A. Raju, Y. Negi, and J. Balakrishnan, "RCS estimation of complex shaped aircraft and RCS reduction using partial RAM coating," *27th Annual Review of Progress in Applied Computational Electromagnetics (ACES)*, Williamsburg, Virginia, pp. 570-575, March, 2011.

[12] K. Mitzner, "Incremental length diffraction coefficients," *Northrop Corporation, Tech. Rep.* AFAL-TR-73-296, 1974.

[13] F. Weinmann, "UTD shooting-and-bouncing extension to a PO/PTD ray tracing algorithm," *Applied Computational Electromagnetics Society (ACES) Journal*, vol. 24, no. 3, pp. 281-293, 2009.

[14] H. Ling, R. Chou, and S. Lee, "Shooting and bouncing rays: Calculating the RCS of an arbitrary shaped cavity," *IEEE Trans. Antennas Propag.*, vol. 37, no. 2, pp.194-205, 1989.

[15] R. Kipp and M. Pavlovic, "Comparison of ray-tracing and MoM RCS solution for large realistic vehicle," *25th Annual Review of Progress in Applied Computational Electromagnetics (ACES)*, Monterey, California, pp. 571-576, March, 2009.

[16] C. Reddy, M. Deshpande, C. Cockrell, and F. Beck, "Fast RCS computation over a frequency band using method of moments in conjunction with asymptotic waveform evaluation technique," *IEEE Trans. Antennas Propag.*, vol. 46, no. 8, pp. 1229-1233, 1998.

[17] Y. Erdemli, J. Gong, C. Reddy, and J. Volakis, "Fast RCS pattern fill using AWE technique," *IEEE Trans. Antennas Propag.*, vol. 46 no. 11, pp. 1752-1753, 1998.

[18] X. Wang, S. Gong, J. Guo, Y. Liu, and P. Zhang, "Fast and accurate wide-band analysis of antennas mounted on conducting platform using AIM and asymptotic waveform evaluation technique," *IEEE Trans. Antennas Propag.*, vol. 59 no. 12, pp. 4624-4633, 2011.

[19] G. Burke, E. Miller, S. Chakrabarthi, and K. Demarest, "Using model-based parameter estimation to increase the efficiency of computing electromagnetic transfer functions," *IEEE Trans. Magn.*, vol. 25, pp. 2807-2809, 1989.

[20] A. Boag, "A fast physical optics (FPO) algorithm for high frequency scattering," *IEEE Trans. Antennas Propag.*, vol. 52, no. 1, pp. 197-204, 2004.

[21] A. Boag and E. Michielssen, "A fast physical optics (FPO) algorithm for double-bounce scattering," *IEEE Trans. Antennas Propag.*, vol. 52, no. 1, pp. 205-212, 2004.

[22] A. Boag and C. Letrou, "Multilevel fast physical optics algorithm for radiation from non-planar apertures," *IEEE Trans. Antennas Propag.*, vol. 53, no. 6, pp. 2064-2072, 2005.

[23] A. Manyas and L. Gurel, "Memory-efficient multilevel physical optics algorithm for fast computation of scattering from three-dimensional complex targets," *Computational Electromagnetics Workshop*, Izmir, Turkey pp. 26-30, 2007.

[24] L. Gurel and A. Manyas, "Multilevel physical optics algorithm for fast solution of scattering

problems involving nonuniform triangulations," *Antennas and Propagation Society International Symposium, IEEE*, Honolulu, Hawaii, pp. 3277-3280. 2007.

[25] M. Stephanson and J. Lee, "Fast physical optics calculation for SAR imaging of complex scatterers," *Antennas and Propagation Society International Symposium, IEEE*, Chicago, Illinois, pp. 1-2. 2012.

[26] O. Bucci and G. Franceschetti, "On the spatial bandwith of scattered," *IEEE Trans. Antennas Propag.*, vol. 35, no. 12, pp. 1445-1455, 1987.

[27] H. Buddendick and T. Eibert, "Acceleration of ray-based radar cross section predictions using monostatic-bistatic equivalence," *IEEE Trans. Antennas Propag.*, vol. 58, no. 2, pp. 531-539, 2010.

[28] F. Catedra, L. Lozano, I. Gonzalez, E. Garcia, and M. Algar, "Efficient techniques for accelerating the ray-tracing for computing the multiple bounce scattering of complex bodies modeled by flat facets," *Applied Computational Electromagnetics Society (ACES) Journal*, vol. 25, no. 5, pp. 395-409, 2010.

[29] Y. Tao, H. Lin, and H. Bao, "GPU-based shooting and bouncing ray method for fast RCS prediction," *IEEE Trans. Antennas Propag.*, vol. 58, no. 2, pp. 494-502, 2010.

[30] W. Gordon, "Far-field approximations to the kirchhoff helmholtz representations of scattered fields," *IEEE Trans. Antennas Propag.*, pp. 590-592, July 1975.

[31] K. Jin, T. Suh, S. Suk, B. Kim, and H. Kim, "Fast ray tracing using a space-division algorithm for RCS prediction," *J. Electromagn. Waves Applicat.*, vol. 20, no. 1, pp. 119-126, 2006.

[32] W. Chew, T. Cui, and J. Song, "A FAFFA-MLFMA algorithm for electromagnetic scattering," *IEEE Trans. Antennas Propag.*, vol. 50, no. 11, pp. 1641-1649, 2002.

[33] CST Microwave Studio 2006B by Computer Simulation Technology [Online]. Available: http://www.cst.com.

Yuyuan An received the B.Sc. degree in Electronic Information Engineering from the School of Electrical Engineering and Optical Technique, Nanjing University of Science and Technology, Nanjing, China, in 2009.

He is currently working towards the Ph.D degree in electromagnetic fields and microwave technology at the School of Electrical Engineering and optical technique, Nanjing University of Science and Technology. Her research interests include antennas, RF-integrated circuits, and computational electromagnetics.

Zhenhong Fan received the M.Sc. and Ph.D degrees in electromagnetic field and microwave technique from Nanjing University of Science and Technology (NJUST), Nanjing, China, in 2003 and 2007, respectively.

During 2006, he was with the Center of wireless Communication in the City University of Hong Kong, Kowloon, as a Research Assistant. He is currently an associate professor with the Electronic Engineering of NJUST. He is the author or coauthor of over 20 technical papers. His current research interests include computational electromagnetics, electromagnetic scattering and radiation.

Dazhi Ding received the B.Sc. and Ph.D degrees in Electromagnetic Field and Microwave Technique from Nanjing University of Science and Technology (NUST), Nanjing, China, in 2002 and 2007, respectively.

During 2005, he was with the Center of Wireless Communication in the City University of Hong Kong, Kowloon, as a research assistant. He is currently an associate professor with the Electronic Engineering of NJUST. He is the author or coauthor of over 30 technical papers. His current research interests include computational electromagnetics, electromagnetic scattering, and radiation.

Rushan Chen received the B.Sc. and M.Sc. degrees from the Department of Radio Engineering, Southeast University, China, in 1987 and 1990, respectively, and the Ph.D degree from the Department of Electronic Engineering, City University of Hong Kong, in 2001.

He joined the Department of Electrical Engineering, Nanjing University of Science and Technology (NJUST) in 1990. Since September 1996, he has been a Visiting Scholar with the Department of Electronic Engineering, City University of Hong Kong, first as Research Associate, then as a Senior Research

Associate, a Research Fellow, and a Senior Research Fellow. From June to September 1999, he was also a Visiting Scholar at Montreal University, Canada. In 1999, he was promoted to Full Professor and Associate Director of the Microwave and Communication Research Center in NJUST, and appointed Head of the Department of Communication Engineering in 2007. He was appointed as the Dean in the School of Communication and Information Engineering, Nanjing Post and Communications University in 2009. In 2011 he was appointed as Vice Dean of the School of Electrical Engineering and Optical Technique, NJUST. His research interests mainly include microwave/ millimeter-wave systems, measurements, antenna, RF-integrated circuits, and computational electromagnetics. He has authored or coauthored more than 200 papers, including over 140 papers in international journals.

Dr. Chen has received 6 prizes. In 2008, he became a Chang-Jiang Professor under the Cheung Kong Scholar Program awarded by the Ministry of Education, China. He was selected as a member of Electronic Science and Technology Group by academic degree commission of the State Council in 2009. He is a Senior Member of the Chinese Institute of Electronics (CIE), Vice-Presidents of Microwave Society of CIE and IEEE MTT/APS/EMC Nanjing Chapter. He serves as the reviewer for many technical journals, and now an Associate Editor for the International Journal of Electronics.